Journal of Fluid Science and Technology

Vol. 3, No. 7, 2008

Fluid Dynamics Study on a Cold Model of Fixed-Bed Fire-Tube Heating Pyrolysis Reactor for Ejection of Solid Char*

Islam M. ROFIQUL**, Hiroyuki HANIU*** and Sangil KIM***

**Department of Mechanical Engineering

Rajshahi University of Engineering & Technology, Rajshahi-6204, Bangladesh

E-mail:mrislam1985@yahoo.com

*** Depatment of mechanical Engineering

Kitami Institute of Technology, Kitami City, Hokkaido 090-8507, Japan

E-mail: harry@mail.kitami-it.ac.jp

Abstract

To innovate an easy and economic way for removal of solid char product from a fixed-bed fire-tube heating pyrolysis reactor the fluid dynamics studies on its cold model are essential. Thus, two types of fluid dynamics experiments have been carried out on a cold model of the pyrolysis reactor: (i) to determine the ejection pressure of the solid char from the reactor, which was carried out with the help of an air compressor and artificial solid char and (ii) to investigate the flow pattern inside the reactor chamber during ejection of char that was conducted by laser Doppler velocimetry (LDV) measurement and flow visualization test. The experimental results show that variation of char ejection pressure with respect to superficial air velocity always follows a polynomial of second-degree. The normalized pressure should be reached to a value about 1.7 with a corresponding normalized superficial air velocity nearly to 1.0, to be started the char product blown out from the reactor model properly. The LDV measurements and visualization test ensure that the spiral char exit port is not able to create a rotary motion inside the reactor chamber during the removal of solid char.

Key words: Fluid Dynamics Study, Cold Model, Fire-Tube Heating Reactor, LDV

1. Introduction

The energy crisis and environmental degradation are the main problems mankind is facing today. These problems owe their origin to a growing population, rapid industrialization and huge quantities of solid refuse, which are generated daily. By the year 2100, the world population is expected to be in excess of 12 billion and it is estimated that the demand for energy will be increased by five times from what it is now. The increasing human population on the earth caused ever-increasing demand of energy. To alleviate part of our energy crisis and environmental degradation, it has become imperative to make use of appropriate technologies for the possible recovery of resources from non-conventional sources, like municipal and/or industrial organic wastes, refused plastics, used tires, etc. The disposal of these non-biodegradable organic solid wastes from human activity is a growing environmental problem for modern society, especially in developing countries.

The pyrolysis of organic solid wastes has received increasing attention since the process conditions may be optimized to produce high energy density liquids, char and gases. In addition, the liquid products can be stored until required or readily be transported to where it can be most efficiently utilized. Tire pyrolysis liquids have been found to have a high gross calorific value (GCV) of around 35-44 MJ/kg, which would encourage their use as replacements for conventional liquid fuels(1-8). In addition to their use as fuels, the liquids have been shown to be a potential source of light aromatics such as benzene, toluene and xylene (BTX), which command a higher market value than the raw oils(1-3, 7, 9). Pyrolytic

*Received 27 May, 2008 (No. 08-0388)
[DOI: 10.1299/jfst.3.826]

char may be used as a solid fuel or as a precursor for activated carbon manufacture(1, 7). Some of the previous research groups(1, 3, 7, 9) studied the composition of evolved pyrolysis gas fraction and reported that it contains high concentrations of methane, ethane, butadiene and other hydrocarbon gases with a GCV of approximately 30-37 MJ/m^3, sufficient to provide the energy required by the pyrolysis process.

The authors of the present paper have developed and operating a fixed-bed fire-tube heating pyrolysis reactor for production of liquid fuels and chemicals from organic solid wastes, whose working principle has been presented elsewhere(10, 11). The fluid dynamic study for solid char removal from the reactor is crucial to be made the system efficient and continuous. To innovate an easy and economic way for removal of char product from the fire-tube heating pyrolysis reactor two types of fluid dynamics experiments have been carried out on its cold model: (i) to determine the ejection pressure of the solid char from the reactor and (ii) to investigate the flow pattern inside the reactor chamber during ejection of char. The first experiment was carried out on the cold model with the aid of an air compressor and artificial solid char while the second was conducted by laser Doppler velocimetry (LDV) measurement and flow visualization test.

2. Material and method for determining the char ejection pressure

2.1 Preparation of artificial char

The size and shape of the solid char products in a pyrolytic reactor are same as of feedstock but it is very fragile and brakes into smaller size pieces by an impulsive force. Its uses as working substance in the present experiment make the laboratory environment dirty and create harmful weather because the pyrolytic char brakes into power by upward impulsive force of compressed air, which is used to push out the char and when it is re-circulated for several experimental runs. Thus, an artificial char was prepared for the experiment by selecting a suitable pulse-husk and crushed it to obtain the shape and size similar to those of the actual char produced from pyrolysis of organic solid wastes. The density of the selected crushed pulse-husk was 70% that of actual char. The pulse-husk was painted black with synthetic paint and hence its density increased to about 95% that of the actual solid char. The painted pulse-husk was air dried and sieved to obtain a similar size range of 3-5mm diameter for pyrolytic char product, which was used well as solid char for the presented investigation.

2.2 Experimental set-up and procedure

The detail drawing of the cold model of the fire-tube heating reactor and schematic diagram of the experimental set-up are presented in Figs. 1 and 2, respectively. The experimental unit consists of six major components: (1) a fixed-bed fire-tube heating reactor chamber made of 10cm diameter, 5mm thick Plexiglas pipe in order to allow complete optical access for naked eye inside observation; (2) a gravity feed type reactor feeder; (3) an air compressor with pressure regulator and flow control valve; (4) char collecting bag made of nylon net with 2mm apertures; (5) an air flow meter with a measuring accuracy of ±1.0 L/min and (6) a multi-tube manometer. At a distance of 3cm from the bottom of the reactor chamber, a distributor plate was fitted to support the char particles and to provide uniform upward flow of air over the cross-section of the reactor. The distributor plate was made of 2.5mm thick aluminum sheet having 3mm diameter 208 holes. Eight equally spaced 10mm diameter aluminum tubes that were treated as fire-tubes were fixed inside the reactor. The height from the distributor plate to the center of the spiral 4cm×4cm char exit port was 24.5cm. The spiral char exit port made the reactor chamber compact and ensured easier char handling. The opening areas of 208 holes in the distributor plate and 4cm×4cm char exit port are 20.35% and 22.14% of the net cross-sectional area of the fire-tube reactor, respectively. The space inside the fire-tube reactor was capable to contain 750gm of solid organic waste feed. The geometric features of the cold model, which were used to fabricate the reactor chamber, are presented in Table 1.

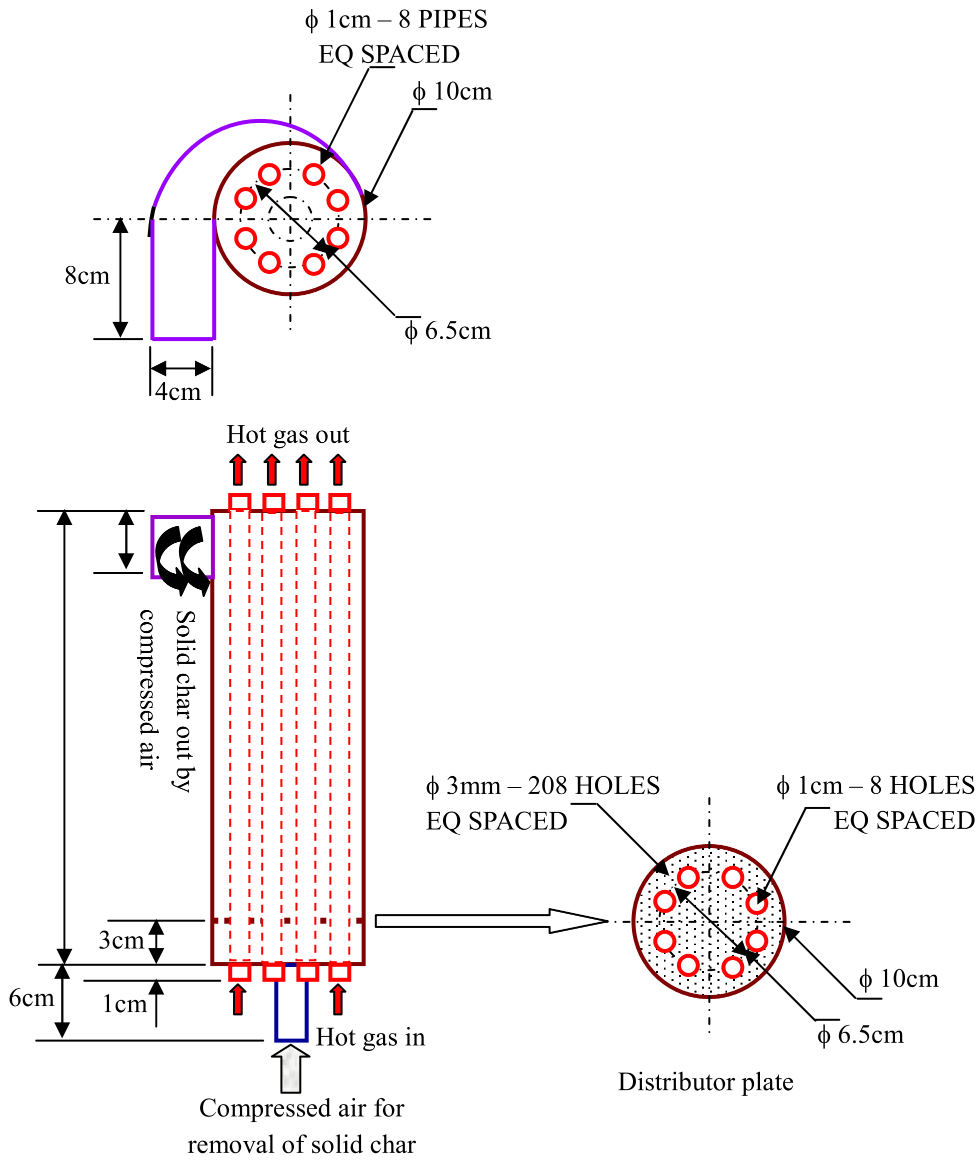

Fig. 1: Detail drawing of the cold model of a fire-tube reactor chamber

Table 1: Main geometric features of the cold model

Inside diameter of the reactor chamber, *d*	10cm
Total height of cylindrical reactor body	30cm
Effective height of reactor, *l*	27cm
Char outlet port dimensions	4cm×4cm
Char exhaust duct length	8cm
Diameter of air inlet bottom pipe	3cm
Number of fire-tubes, n	8
Height of a fire-tube	33cm
Outside diameter of the fire-tube, d_1	1cm
Diameter of fire-tubes positioning circle	6.5cm
Position of the distributor plate from the bottom of the reactor chamber	3cm
Number of holes in the distributor plate	208
Diameter of each hole	3mm
Area of the holes in percentage of cross-sectional area of the fire-tube reactor	20.35%
Cross-sectional area of char exit port	22.14%

It was found that 56-68wt% of solid organic waste feed are decomposed during pyrolysis reaction *i.e.* char yields varies from 32-44wt%(12). During experimental runs, by the action of gravity force four quantities of 262.50, 300, 337.50 and 375 (±2.0) gm of char sample, which were 35, 40, 45 and 50wt% of 750gm waste feed, respectively, were supplied from the feeder into the reactor chamber by opening the feed control valve. The char was pushed out from the reactor chamber with the aid of compressed air supplied from the air compressor by opening char exit port. A flow control valve regulated the flow of air from the compressor while the compressor pressure was maintained constant at 10 bars. Char was collected in the char collection bag. The pressure on the upper and lower sides of the distributor plate was measured by a multi-tube manometer. The pressure readings were taken by varying the flow of air for both of char full and empty reactor conditions. Each experiments was repeated at least five times. The superficial air velocity (velocity of air in empty reactor chamber) in the fire-tube reactor chamber was calculated by the Eq. 1. The superficial air velocity in m/sec,

$$U_f = \left(\frac{1}{\frac{\pi d^2}{4} - \frac{n \pi d_1^2}{4}} \right) \times \left(\frac{Q}{1000 \times 60} \right) \qquad (1)$$

Where, volume flow rate of air, Q is in L/min; internal diameter of the reactor cylinder, d = 0.10m; outer diameter of fire-tube, d_1 = 0.01m; number of fire-tubes, n = 8.

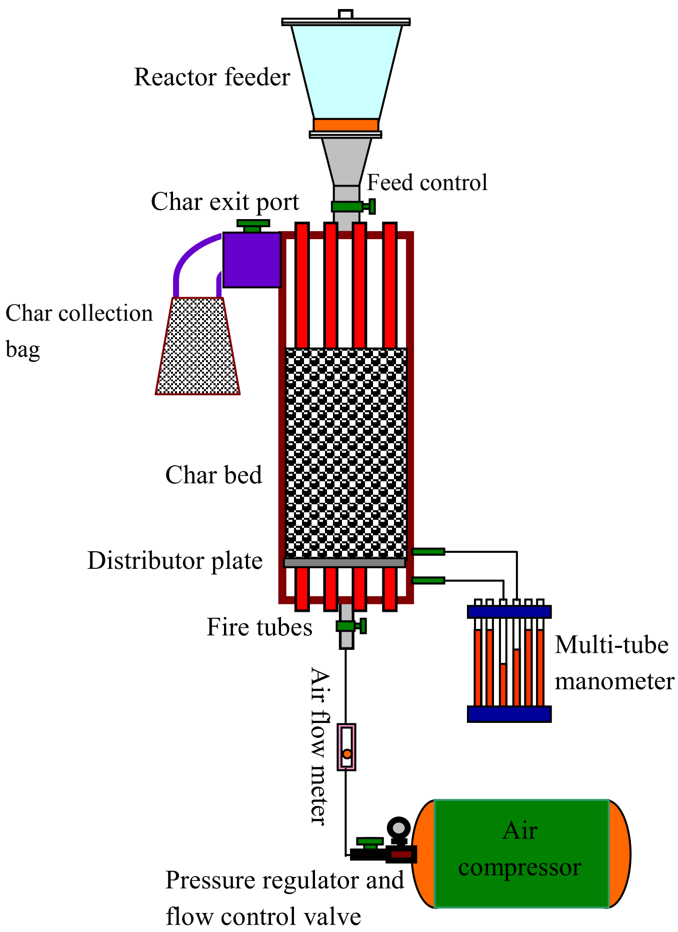

Fig. 2: Schematic diagram of a cold model fixed-bed fire-tube heating pyrolysis system for fluid dynamics study to determine char ejection pressure

2.3 Results and discussions

The mean value of five sets of repeated experimental data for pressure on the upper and lower side of the distributor plate corresponding to different superficial air velocity are presented in Fig. 3 for both of empty and char full conditions. The Fig. 3 shows that the value of pressure on the lower side of the distributor plate is always higher than that on the upper side of the plate for both cases. This is due to the fact that the flow of air is somewhat stagnant for the presence of distributor plate, which reduces air flow area 79.65%. This results in decrease in air flow and increase in pressure on the lower side of the plate than those on the upper side. It is important to note that char ejection pressure is normalized by downward pressure due to weight of the char for full char condition (with 375gm char) on the distributor plate while the corresponding superficial air velocity is normalized by the air velocity at which char particles starts to blow out. The normalized pressure on the upper and lower side of the distributor plate with respect to different values of normalized superficial air velocity for the four selected char weight are presented in Figs. 4 and 5, respectively. All of the Figs. 3-5 show that the pressure increases with the increase of superficial air velocity following a polynomial of second-degree (shown below) for both of empty and char full conditions.

$$P_n = a_0 + a_1 U_{fn} + a_2 U_{fn}^2 \qquad (2)$$

It is obvious that the pressure at char full condition is higher than that of empty condition for a particular air velocity. It is seen from the Figs. 3-5, when the normalized pressure reaches to a value about 1.7 for full char condition (with 375gm char) with a corresponding normalized superficial air velocity nearly to 1.0, the char starts to blow out from the reactor model properly. After this stage, the flow of air is increased at the same rate and the char particles blow out continuously while the pressure increases slightly due to corresponding reduction of char weight. When all of the char particles are ejected completely *i.e.* the reactor chamber becomes empty the P_n versus U_{fn} curves merge with those obtained at empty condition of the reactor.

The Eq. (2) can be reduced to find a least-square straight line on P_n versus U_{fn} plane through the experimental data. The best values of the regression coefficients (coefficients of the linear least-square fit line), a_0, a_1 and a_2 can be calculated from the well known least

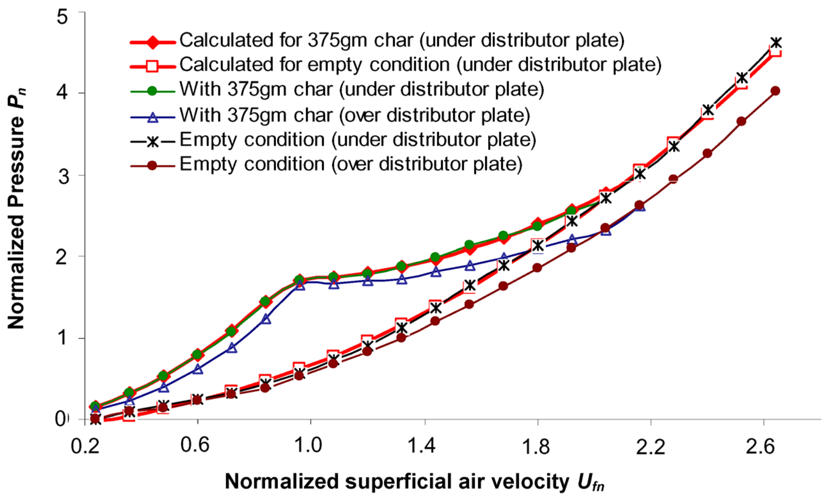

Fig. 3: Pressure difference on upper and lower side of the distributor plate for both of empty and char full conditions with calculated values

square method. Fig. 3 also shows that the calculated data fit fairly well with those obtained from experiments for both of empty and char full conditions. From the naked eye observation, it was also found that the char particles did not rotate around a vertical axis during ejection time, although the ejection port was of spiral shape. Thus, it could be realized that there was no rotational flow of air inside the reactor chamber. The char particles just took a turning motion toward the port opening on vertical plane. The turning started close to the char exit port which was in-between 190-210mm from the distributor plate. To be sure about the flow pattern inside the reactor chamber, the LDV measurement has been carried out, which is described in the following sections.

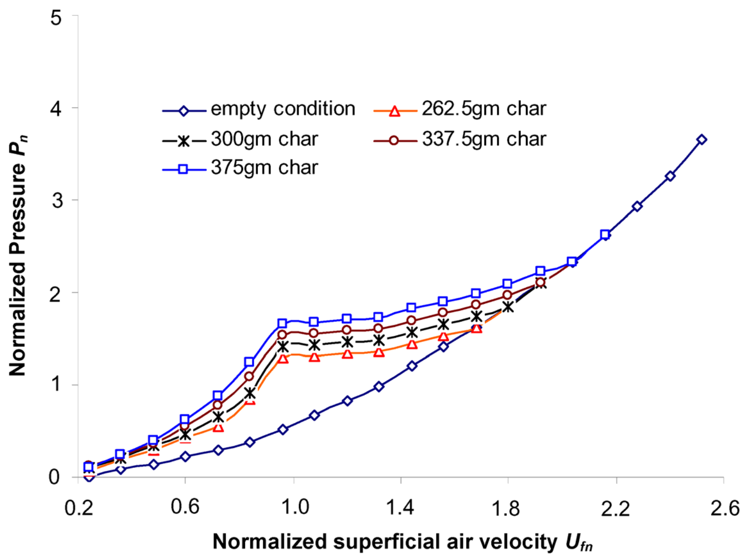

Fig. 4: Pressure difference on upper side of the distributor plate, P_n versus superficial air velocity, U_{fn} curves for different char weight

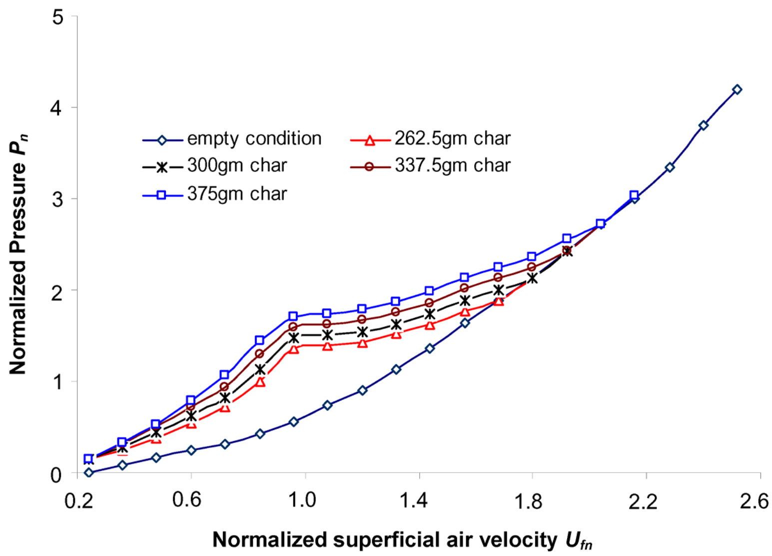

Fig. 5: Pressure difference on lower side of the distributor plate, P_n versus superficial air velocity, U_{fn} curves for different c

3. Material and method for investigating the flow pattern

3.1 Experimental set-up and procedure

The schematic diagram of the experimental set-up for fluid dynamics study to investigate the flow pattern inside reactor cylinder is presented in Fig. 6. The experimental unit consists of five major components: (1) the Plexiglas pipe fabricated fire-tube reactor chamber in order to allow complete optical access for measurement through LDV and flow visualization test; (2) a water pump; (3) LDV with NEC He-Ne laser source; (4) data acquisition and processing system; (5) a 1.0m×0.33m×0.4m size water tank. The velocity measurements have been performed by LDV, which ensures non-intrusivity, high spatial and temporal resolution. The system used was a dual-beam, backscatter LDV device operating with a maximum power of 10 mW Spectra-Physics Helium-Neon laser. Sensitivity to flow direction was provided by a frequency shifting of 158 kHz operated by a Bragg cell, where the laser wavelength was 632 nm. The Doppler signals were monitored by a 58N10PDA Dantec processor interfaced with a PC through a DMA modulus. Small amount of latex particles were used as seeding/tracer particles for the measurement. The cylindrical shape of the reactor body did not allow water velocity measurements closer than 5mm from the wall, although the flow pattern in the central region was resolved successfully along radial directions. The LDV probe was mounted on a 3-D traversing mechanism with 0.1 mm accuracy, allowing separate measurements of the X and Y-velocity components from the side of the cylindrical reactor body. The two velocity components were measured at four sections of 100mm, 150mm, 200mm and 210mm distance from distributor plate. The refractive index of water and Plexiglas affected both of the refraction angles and wavelength of the laser beam that were cancelled out and hence only the position of the focus point was considered in calculating the velocity by the LDV measurement. The position of the reactor chamber shown in Fig. 6 is 0-degree position.

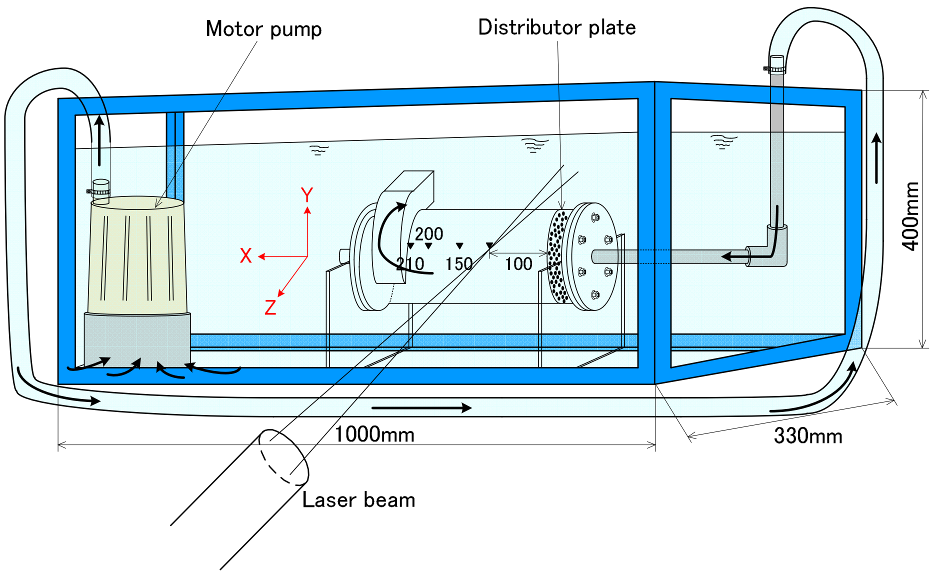

Fig. 6: Schematic diagram of the experimental set-up for LDV measurement

The laser source was proceeded transverse direction and velocity data were taken after 10mm interval for all of the four selected sections. For time mean velocity, we tried to get statistically stable result. Therefore, we took longer time sampling, which was given less scattered result at each location. We repeated sufficiently and found almost same result. The reactor chamber rotated anticlockwise through 90 degree and the same measurements as of

0-degree position were conducted. The data were collected for both with and without placing the fire-tubes inside the reactor chamber. Reactor cylinder positions for LDV measurements at 0-degree and 90-degree are presented in Figs. 7 and 8, respectively. It is obvious that the volume flux at each section of the reactor cylinder remains constant and it was verified by using the measured velocity at different sections. The method adopted to calculate the total flux at a particular section is presented in Fig. 9 and Eq. (3) was used to calculate the total flux.

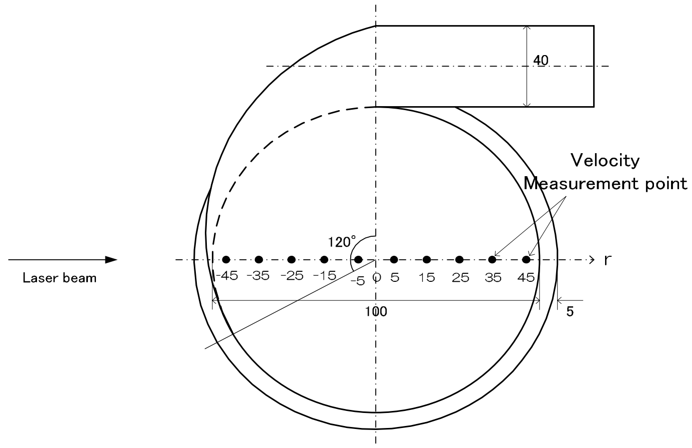

Fig. 7: 0-degree position of reactor cylinder for X and Y-velocity component measurements

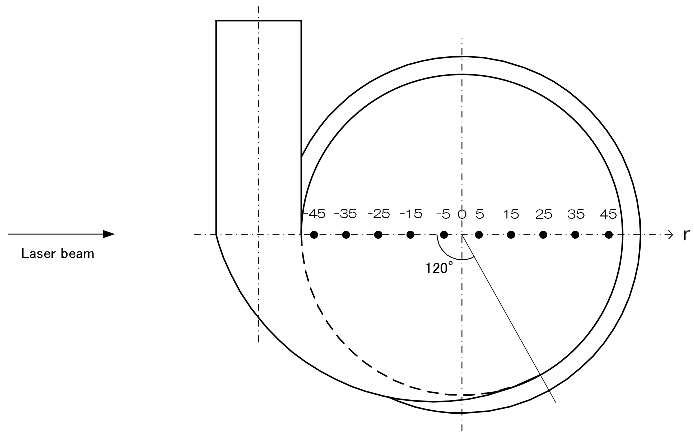

Fig. 8: 90-degree position of reactor cylinder for X and Y-velocity component measurements

Total flux at a particular section, $Q_T = Q_a + Q_b + Q_c + Q_d + Q_e$ (3)

Where, $Q_a = Q_{00\text{-}1} + Q_{90\text{-}1} + Q_{00\text{-}10} + Q_{90\text{-}10}$
$Q_b = Q_{00\text{-}2} + Q_{90\text{-}2} + Q_{00\text{-}9} + Q_{90\text{-}9}$
$Q_c = Q_{00\text{-}3} + Q_{90\text{-}3} + Q_{00\text{-}8} + Q_{90\text{-}8}$
$Q_d = Q_{00\text{-}4} + Q_{90\text{-}4} + Q_{00\text{-}7} + Q_{90\text{-}7}$
$Q_e = Q_{00\text{-}5} + Q_{90\text{-}5} + Q_{00\text{-}6} + Q_{90\text{-}6}$

For instance, flux through the shaded area, $Q_{00\text{-}8} = A_{00\text{-}8} \times V_{00\text{-}8}$ and the average velocity at a particular section has been calculated by the following equation:
$V_{average} = Q_T/A$, where A is the cross-sectional area of the reactor chamber.

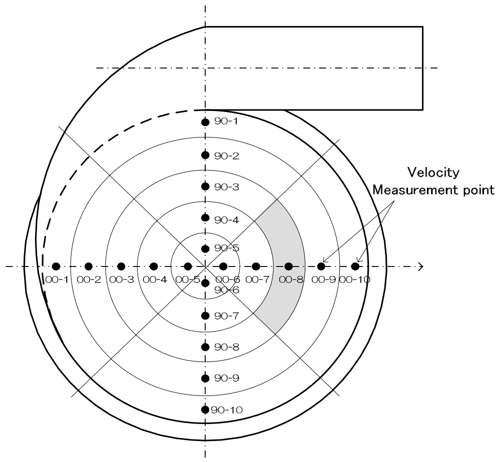

Fig. 9: Representation of method adopted for flux calculation

3.2 Results and discussions

The Eq. (4) gives the total flux at sections 100, 150, 200 and 210mm are 0.00035, 0.00036, 0.00035 and 0.00035 m^3/sec, respectively. It is seen that the total flux throughout the cylinder is almost constant. This result confirms the accuracy of the LDV measurements. The Reynolds Number for the LDV measurement was 12,130 without fire-tubes, which was in the range of that values for real char removal situation. The velocities obtained by LDV measurements are presented in Figs. 10-14. Figs. 10-12 show that the velocity profiles at sections 100 and 150mm from the distributor plate are in wave shape instead of the obvious parabolic shape in general pipe flow case and more or less symmetric on both sides of the centerline *i.e.* X-axis of the cylinder. This type of shapes is due to the presence of 1cm diameter 8 blind spaces in the distributor plate (Fig. 1), which was placed in the upstream. These spaces are used for placing fire-tubes. When the experiment was conducted without fire-tubes, the spaces was blind *i.e.* did not contain small (3mm diameter) openings. Under this situation the flow obstructed by the blind spaces and became fast around the spaces and

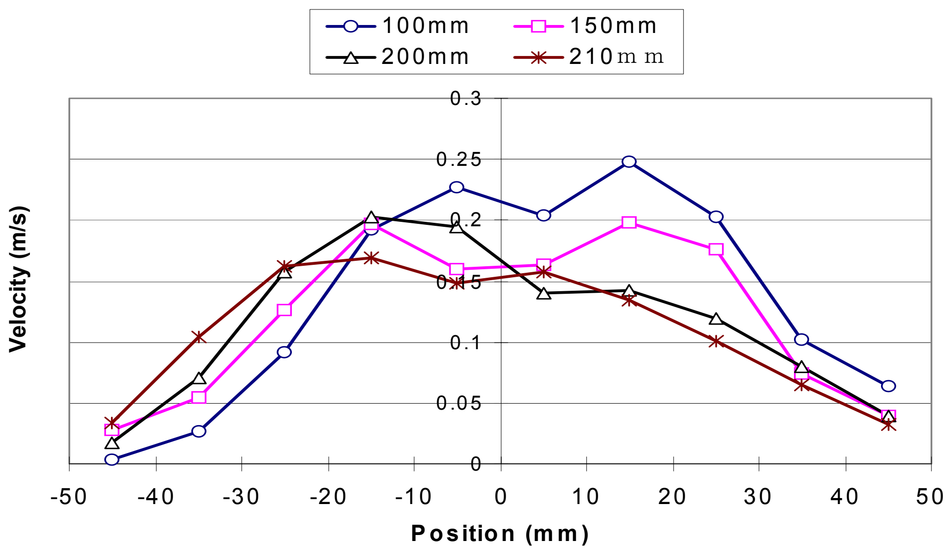

Fig. 10: X-direction velocity for 0-degree position and without fire-tube conditions

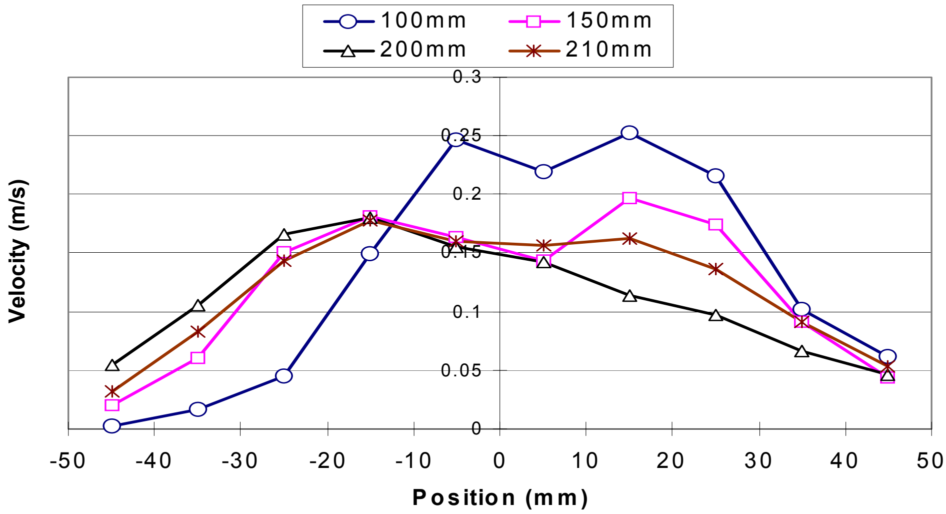

Fig. 11: X-direction velocity for 90-degree and without fire-tube conditions

also merges downstream of the distributor plate. The non-smoothness of the velocity profile or a little fluctuation in velocities is also due to the presence of distributor plate in the upstream. At sections 200 and 210mm from the plate, the velocity profile changes and the X-component velocities of the left side of X-axis are comparatively become higher than those of the right side, because of the left side upper and lower positioning of the char exit port. This happens for both cases with and without placement of fire-tubes inside the reactor cylinder. The Figs. 13-14 show that the Y-component velocity always positive values *i.e.* upward turning of the fluid flow due to upper position of the char exit port. The Y-component velocities at sections 100 and 150mm almost same on both sides of the cylinder centerline while at sections 200 and 210mm its values for left side become higher than those of the right side for both cases of with and without fire-tubes inside the cylinder. The velocity profiles with and without placement of fire-tubes in the reactor cylinder almost same but magnitude of velocity with tubes is 1.1 times higher than that obtained without tubes due to the fact of area reduction for fluid flow.

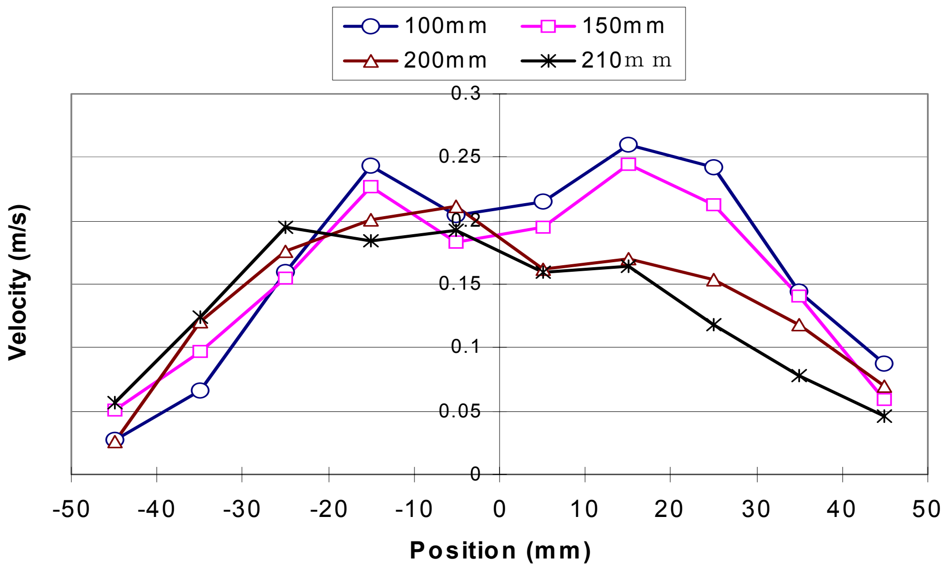

Fig. 12: X-direction velocity for 0-degree and with fire-tube conditions

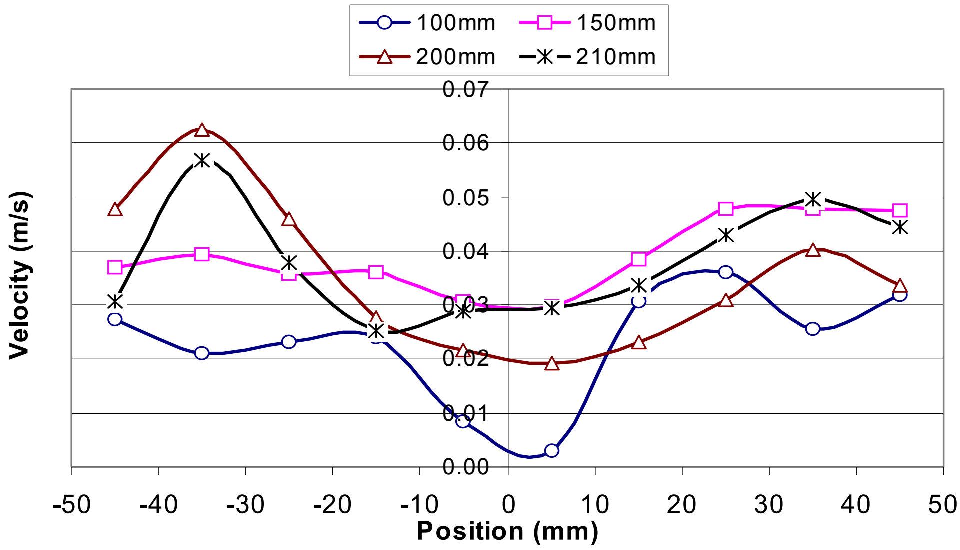

Fig. 13: Y-direction velocity for 0-degree and without fire-tube conditions

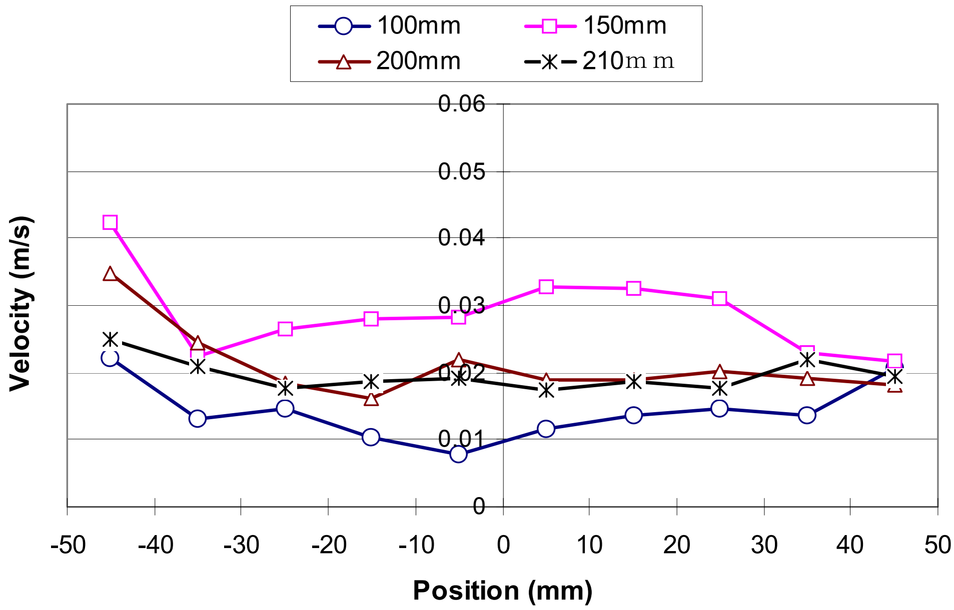

Fig. 14: Y-direction velocity for 0-degree and with fire-tube conditions

The above results do not bear any significance for the presence of a rotational flow inside the cylinder. To be more sure about the flow pattern inside the cylinder a visualization test has been carried out taking photo and movie of the flow inside the cylinder without fire-tubes. Three threads of different colors were used for this investigation. It was found that the flow was more or less straight up to 190mm from the distributor plate and then took a turning toward the port opening in-between 190-210mm.

4. Conclusions

- The variations of char ejection pressure with respect to superficial air velocity always follow a polynomial of second-degree for the presented fixed-bed fire-tube heating reactor system.

- The normalized pressure should be reached to a value about 1.7 with a corresponding normalized superficial air velocity nearly to 1.0, to be started the char product blown out from the reactor chamber properly.
- The char particles just take a turning toward the char exit port.
- The LDV measurements and visualization test ensure that the spiral char exit port is not able to create a rotary motion inside the reactor chamber during removal of char. Thus less amount of power is required for the present char removal system than that of the case where rotational flow is exists.

Acknowledgement

The first author (M. Rofiqul Islam) would like to express his sincere gratitude and thanks to the Japan Society for the Promotion of Science (JSPS) for financial support during his research period in Japan under ID No.: UGC-10632. The technical assistance for fabricating the cold model supported by Mr. Yoshiro OBATA of Fluid Mechanic Laboratory in Kitami Institute of Technology of Japan, is gratefully acknowledged.

References

(1) Rodriguez IM, Laresgoiti MF, Cabrero MA, Torres A, Chomon MJ, Caballero BM. Pyrolysis of scrap tires. *Fuel Process Tech* 2001;72:9–22. [and references therein]

(2) Laresgoiti MF, Caballero BM, De Marco I, Torres A, Cabrero MA and Chomon MJJ. Characterization of the liquid products obtained in tire pyrolysis. *J. Anal. Appl. Pyrolysis* 2004;71:917–934.

(3) Gonzalez JF, Encinar JM, Canito JL, Rodriguez JJ. Pyrolysis of automotive tire waste. Influence of operating variables and kinetic study. *J. Anal. Appl. Pyrolysis* 2001;58–59:667–683 [and references therein].

(4) Diez C, Martinez O, Calvo LF, Cara J, Moran A. Pyrolysis of tires. Influence of the final temperature of the process on emissions and the calorific value of the products recovered. *Waste Management* 2004;24:463-469.

(5) Dai X, Yin X, Wu C, Zhang W, Chen Y. Pyrolysis of waste tires in a circulating fluidized-bed reactor. *Energy* 2001;26:385-99.

(6) Pakdel H, Pantea DM, Roy C. Production of *dl*-limonene by vacuum pyrolysis of used tires. *J. Anal. Appl. Pyrolysis* 2001;57:91–107.

(7) Cunliffe AM, Williams PT. Composition of oils derived from the batch pyrolysis of tires. J Anal Appl Pyrol 1998;44:131–152. [and references therein]

(8) Roy C, Chaala A, Darmstadt H. Vacuum pyrolysis of used tires End-used for oil and carbon black products. J. Anal. Appl. Pyrolysis 1999;51:201–21.

(9) Williams PT, Brindle AJ. Aromatic chemicals from the catalytic pyrolysis of scrap tires. *J Anal Appl Pyrolysis* 2003;67:143–164.

(10) Islam MR, Haniu H, Rofiqul ABM. Limonene-rich liquids from pyrolysis of heavy automotive tire wastes. *Journal of Environment and Engineering* 2007;2(4):681-695.

(11) Islam MR, Tushar MSHK, Haniu H. Production of liquid fuels and chemicals from pyrolysis of Bangladeshi bicycle/rickshaw tire wastes. *J Anal Appl Pyrolysis* 2008;82:96–109.

(12) Islam MR, Haniu H and Beg MRA. Pyrolysis kinetics behavior of solid tire wastes available in Bangladesh. *Waste Management,* 2008;XXX:XXX-XXX (**Article in press and available: http://www.sciencedirect.com/science/journal/0956053X**).